The new Spaghetti Calorimeter of the H1 Experiment

Marc Weber[a] representing the H1 collaboration

[a]DESY, Notkestraße 85, D-22603 Hamburg, Germany.

The H1 collaboration is building a new calorimeter which will be installed in the backward scattering region of the H1 detector in the winter shut-down 1994/95. The calorimeter consists of 0.5 mm diameter scintillating fibers embedded into lead plates. The lead to fiber ratio is 2:1. The main design goals for the calorimeter are an energy resolution of better than 2% for 30 GeV electrons and a geometric acceptance up to electron scattering angles of 2.5° with respect to the beam pipe. The design and the construction of the calorimeter is reviewed and the performance of final detector modules in test measurements is presented.

1. INTRODUCTION

The new accelerator ring HERA at DESY collides 27 GeV electrons or positrons with 820 GeV protons. HERA is the ideal tool to study electron–proton reactions at high values for the four-momentum transfer variable Q^2 which have not been accessible to fixed target experiments. Due to the large proton momentum the event particles are boosted in the proton direction – the forward direction. Consequently the instrumentation of the H1 detector is asymmetric as can be seen from Figure 1, where a standard deep inelastic scattering event is shown. The electron beam enters the detector from the left, the protons from the right side. The scattered electron is visible as an isolated track in the central tracking detectors and as an energetic cluster in the backward electromagnetic calorimeter (BEMC). The struck parton has fragmented into a jet of particles directed into the forward region.

With the growing interest in low x physics [1] an improved measurement of events where the electron strucks a soft parton inside the proton and the generated particles might be boosted in the backward (electron) direction was requested [2].

The H1 collaboration has therefore started an ambitious upgrade programm of the backward part of detector. In particular the existing lead-scintillator-sandwich calorimeter, the BEMC, will be replaced during winter-shutdown 1994/95. The required performance of the new calorimeter and its construction techniques will be described below.

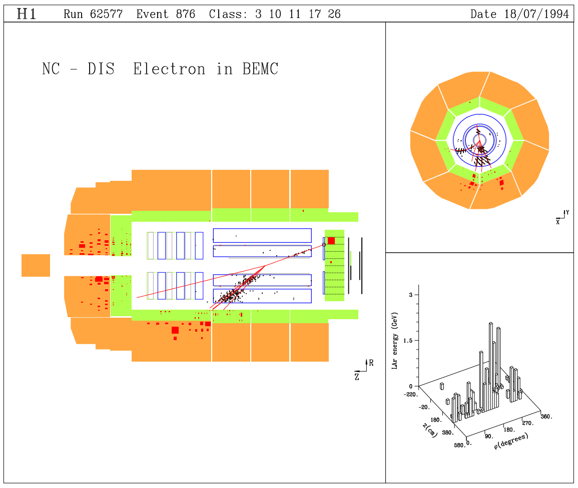

Figure 1. A deep inelastic scattering event recorded with the H1 detector with the scattered electron observed in the backward calorimeter (on the right side of the detector).

2. PHYSICS MOTIVATION

The main features of the new calorimeter in comparison to the BEMC are the following:

- A large geometric acceptance covering electron scattering angles larger than 2.5° which will extend the measurements of the proton structure function F_2 down to very low x values.
- A much improved electromagnetic energy resolution of better than 2 % for electron energies of 30 GeV in combination with an absolute energy calibration of 0.5% and a spacial homogeneity close to 2 % is essential to keep the systematic uncertainties of the F_2 measurements in the range of 5 - 10% [3].
- A position resolution in the millimeter range which corresponds to an angular resolution of the scattered electron of a few mrad.
- A reliable electron–pion separation is needed to suppress background events from photoproduction which are several orders of magnitudes more abundant than deep inelastic scattering events. Pions from photoproduction may thus be a source of fake electrons in the backward region.
- A time resolution of less than 1 ns independent of the particle energy i. e. for high energetic electrons, interacting pions as well as for minimum ionizing particles to suppress upstream proton background already at the first trigger level.
- The measurement of hadrons which allows us to determine the kinematic variable y without using the electron information. This offers the possibility to make cross checks and to identify radiative events with an additional photon radiated by the initial or final state electron.

A summary of the design characteristics is given in Table 1.

Table 1
Design goals

Acceptance	$153° < \theta < 177.5°$
σ /E	$7\%/\sqrt{E} \oplus 1\%$
e/π separation	$\epsilon_e/(1-\epsilon_\pi) > 100$
Time resolution	< 1 ns
Position resolution	a few mm
Angular resolution	2 mrad
Absolute calibration	0.5 %

3. DESIGN AND CONSTRUCTION

Two different calorimeter types were seriously considered to be good candidates to fulfil the requirements discussed above — a lead fluoride cristal calorimeter and a spaghetti calorimeter (Spacal). Prototypes for both options were built and investigated in detail [4,5]. The main reason to favour a spaghetti type calorimeter were the high cost and the restricted hadronic response of the cristals.

The exact position of the Spacal within the H1 detector is shown in Figure 2.

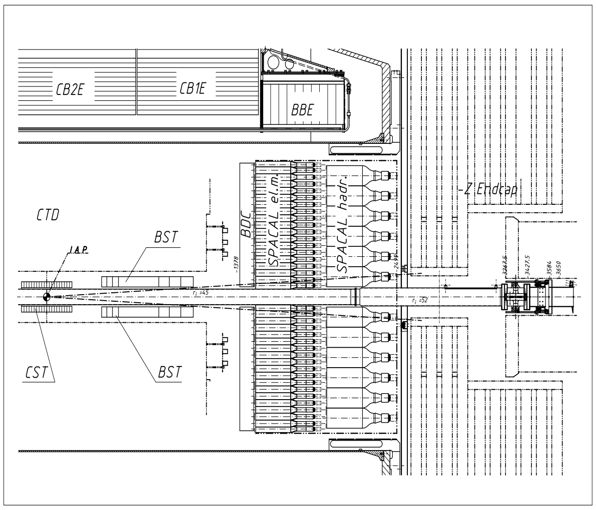

Figure 2. Extended view of the backward region of the H1 detector showing the two Spacal sections.

The two different sections of the Spacal – electromagnetic and hadronic ones – provide the longitudinal segmentation useful for particle identification. The fiber bundels, light mixers and photomultipliers of the electromagnetic section are directly in front of the hadronic one and have to be kept as compact as possible. This report will concentrate on the description of the electromagnetic section, which performs the main task of the Spacal, the precise measurement of the scattered electron.

3.1. Submodule production

The basic unit of the electromagnetic calorimeter is a block of 52 lead plates (see Figure 3), called a submodule. Each lead plate has 90 grooves with scintillating fibers put into it. The fibers are grouped into two bundles with a length of 80 mm held in a bundling frame. The bundle ends are coupled by an air gap of 0.3 mm to the light mixers glued to photomultipliers (not shown in the figure). The standard cell size of the electromagnetic section is $40.5 \times 40.5 \times 250$ mm^3.

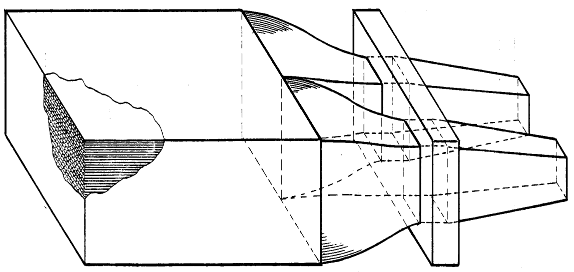

Figure 3. Schematic view of a submodule, the smallest detector unit.

The diameter of the scintillating fibers is 0.5 mm, the lead to fiber volume ratio of the detector is 2:1. Due to the small fiber diameter a high sampling frequency is obtained which allows us to obtain the required energy resolution with a sampling term close to $7\%/\sqrt{E(\mathrm{GeV})}$. The choice of the lead to fiber ratio is a compromise between aiming for an even smaller sampling term or for a more compact calorimeter. Having chosen the fiber diameter and the lead to fiber ratio, the radiation length and the Molière radius of the Spacal are 0.91 and 2.55 cm, respectively. A summary of the main construction parameters is given in Table 2.

In Figure 4 the profile of the lead plates and the fiber position in the plates is shown. The lead plates are produced with a special rolling machine at DESY constructed using the experience of [6]. The quality of the mechanical tolerances of the plates is essential for the performance of the detector. The height of our lead plates is constant to a precision of a few microns. This is at the limit of what is technically realizable today.

Various fibers from different producers were studied with detailed β–source scans [9,10]. The most important fiber properties were a long attenuation length to avoid a signal dependence on the position of the shower maximum, small light yield fluctuations from fiber to fiber which compromise the constant term of the energy resolution and sufficient radiation hardness. Our final choice was the fiber type BCF-12 from BICRON.

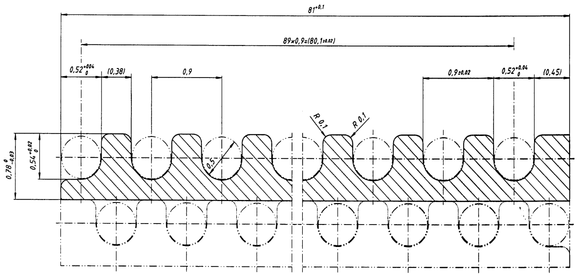

Figure 4. Front view of a lead plate with the grooves for 0.5 diameter scintillating fibers.

A compilation of the results for two different fiber types is shown in Figure 5. For these measurements the fiber length was 30 cm. A considerable increase of the light yield and the attenuation length is observed for fibers mirrored at the end opposite to the photomultiplier. The measured attenuation length is close to three meter for BCF-12 fibers which is largely sufficient for our detector. For all measurements the scintillation light reflected by the cladding of the fiber, which has an attenuation length considerably shorter than the core light, was absorbed by

Table 2
Construction parameters

	Electromagnetic section	Hadronic section
Fiber diameter	0.5 mm	1.0 mm
Lead/fiber ratio	2 : 1	4 : 1
Number of channels	1192	120
Size of standard cell	40.5×40.5 mm^2	120×120 mm^2
Radiation length	0.91 cm	-
Interaction length	25 cm	20 cm
Active length	25 cm	25 cm
Molière radius	2.55 cm	-

a strip of black paint at the fiber end near the photomultiplier.

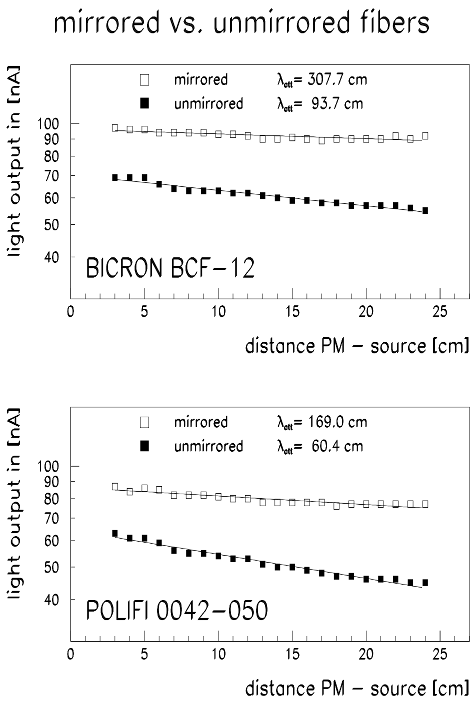

Figure 5. Light yield and attenuation length measurements for two different fiber types, both with and without mirrored fiber ends.

In the following, the main steps of the submodule production are summarized: The mirrored fibers are put into the grooves of the lead plates. The fibers are fixed in the grooves by a thin strip of acrylic glue near the front side of the lead plate. At the PMT side an approximately 1 cm wide strip of black epoxy glue absorbs the cladding light of the fibers and gives mechanical stability. After the preparation of 52 plates, the plates are put into a stacking form, which is then pressed horizontally and vertically with a weight of 1.5 tons. This procedure avoids the uncontrolled deformation of the final detector after its assembly. The stacked lead plates are then stabilized by a layer of 60 μ thick tape surrounding the module. Last, the fiber ends are bundled and glued together with blackened epoxy glue.

3.2. Supermodule production

Eight submodules are combined to form a 16–channel supermodule. By selecting submodules with matching geometrical tolerances, the module cross section of 162.6×162.6 mm^2 is kept within a typical tolerance of 0.1 mm. Next, the back side of the supermodule with the fiber bundles is machined to form a flat optical surface. The supermodule is wrapped in two more layers of tape similar to the submodules. The supermodule production is completed by adding a housing which contains 16 light mixers and PMTs to the machined fiber bundles. A high voltage distribution board and a light calibration module are mounted at the back of the PMT housing.

In Figure 6 a block of four supermodules together with a PMT housing and one of the PMTs on the top of the detectors is shown. The submodule structure of the detector is clearly visible from the front side.

3.3. Channeling

An intrinsic property of all scintillating fiber calorimeters is the channeling effect – the signal dependence on the angle between the impinging particle direction with reference to the fiber orientation. The most extreme scenario is a particle traveling along a fiber with zero inclination and thus producing significantly more light than a particle inside the lead.

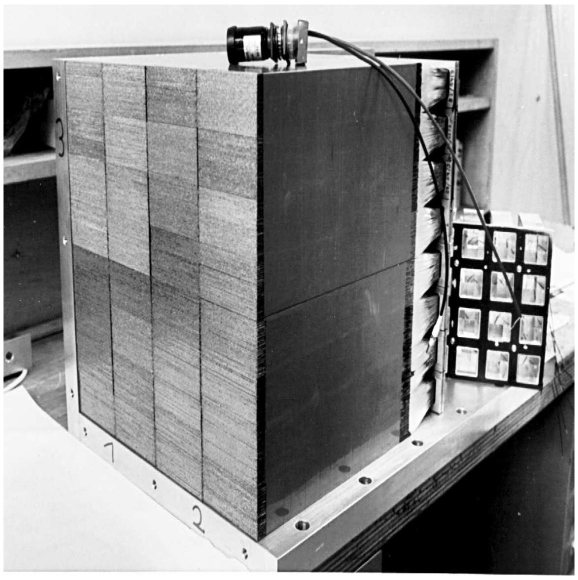

Figure 6. An array of four supermodules.

While this case is not relevant for the H1 Spacal which is an end cap detector, channeling may also occur at angles larger than 0°. This is illustrated in Figure 7.

The particle represented by the arrow on the left side corresponds to the energy spectrum shown in the left histogram. Due to its incidence angle this particle traverses a reasonable mixture of lead and fibers.

In contrast, the particles on the right side, may pass lead only or they may predominantly cross fibers. With a beam of particles entering the calorimeter at this critical angle, the energy spectrum shown in the right histogram is obtained. A double structure is visible, which corresponds to a significantly lower energy resolution.

To reduce any channeling effects in our calorimeter, we vary the submodule orientation depending on their detector position in a way that critical angles are avoided. Thus the supermodules may contain vertically or horizontally stacked submodules or both.

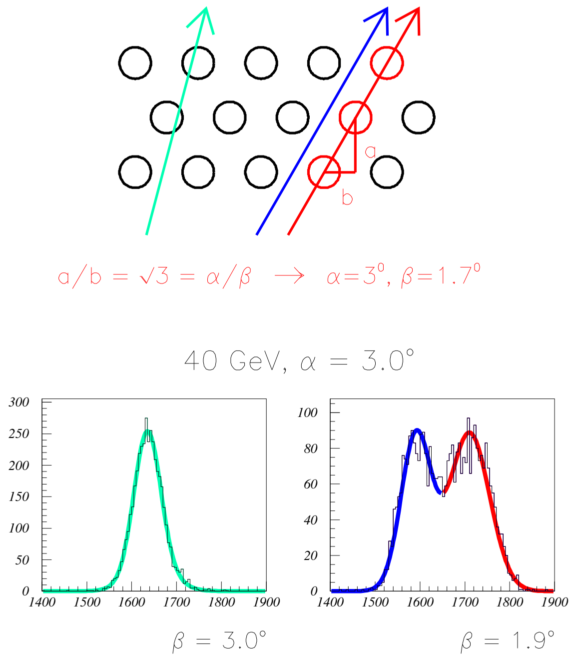

Figure 7. A schematic demonstration of the channeling effect. The angles α and β correspond to the vertical and horizontal inclination of the detector axis with reference to the beam.

3.4. Detector assembly

The r–ϕ view of the Spacal is shown in Figure 8. The circle in the center of the plot represents the beam pipe, which is surrounded by a special module, the insert. The main part of the Spacal is built up of 60 supermodules. At the outer borders a number of special border modules were constructed to minimize the gaps due to the round shape of the detector. The detector itself is contained in an 8 mm thick aluminium vessel.

To install the Spacal around the beam pipe, the modules above the beam pipe can be removed. These modules are hold by four 2 ×25 μm thick steel bands fixed at the top of the detector. Thus these modules will not put any pressure on the insert and consequently the HERA beam pipe.

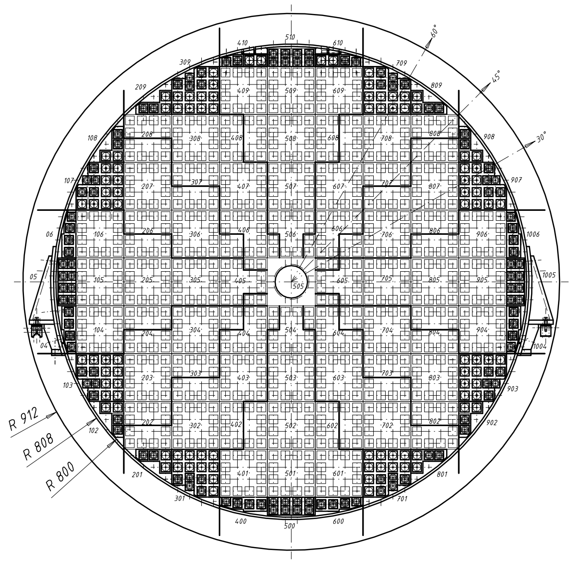

Figure 8. The r–ϕ view of the Spacal.

4. THE HADRONIC SECTION

The hadronic section of the Spacal is built using the same techniques as for the electromagnetic one. Its main purpose is to improve the measurement of hadrons to provide a complementary determination of the kinematic variables y and Q^2 and to suppress photoproduction background events by improving the electron–pion separation. Due to the limited space available for both sections, the hadronic section is only 1.2 interaction lengths deep. The number of interaction length of both calorimeter sections is 2.2 Λ.

For the hadronic section the lead to fiber ratio is 4:1. The same fiber type as for the electromagnetic section was used but with a fiber diameter of 1.0 mm. The hadronic section consists of 120 standard cells with a cross section of 12 × 12 cm^2.

5. PHOTOMULTIPLIERS AND CALIBRATION SYSTEM

The light readout system of the Spacal has to be operated within a magnetic field of approximately 1.0 T. Thus photomultipiers with a standard dynode structure can not be used. A high gain, a low noise level to be sensitive to minimum ionizing particles and a very precise timing are important design goals of the detector. This excludes the use of photodiodes compared to the current BEMC. Our choice was the fine–mesh–multiplier R5505 from Hamamatsu [7,8]. Within a magnetic field of 1.2 T this multiplier achieves a gain of typically 10^4, approximately a factor 100 less than with no field. The gain dependence on the magnetic field as well as the cathode uniformity with and without field of all multipliers have been investigated in detail. These measurements served as quality control and did determine the final PMT position inside the detector.

The short term stability of the photomultiplier gain is monitored by a light calibration system situated at the back side of the calorimeter. Light from two different LEDs is fed through light guiding fibers into the light mixers. The stability of the LED light ouput itself is measured by additional photodiodes. The system will also provide the initial timing adjustment of all detector channels.

6. HIGH VOLTAGE SUPPLY

The high voltage of the photomultipliers is controlled by 16-channel HV–boards following the design of [13]. Each board is supplied by one global high voltage but the different channels may be regulated individually via an opto–coupler within a range of 360 Volts. Thus by means of a bus system the number of HV cables is reduced to 75.

7. ELECTRONICS

The photomultiplier signal is integrated by an emitter–follower positioned inside the housing tube of the PMT together with the high voltage divider. The detector signal is then distributed into the readout system and the trigger branch. The readout is performed by an analog card with shaping and sample/hold functions followed by the standard H1 calorimeter readout chain [14].

The trigger branch signal enters a Pole–Zero–Compensation circuit followed by a Constant Fraction Discriminater which allows us to compare the time of flight of the calorimeter particles with the nominal collision time of genuine electron–proton events. For 'in–time' events a cluster search is performed by the 'Inclusive Electron Trigger'. The 'Inclusive Electron Trigger' compares the total energy of all possible combinations of four neighbouring cells to different energy thresholds. This provides the trigger for deep inelastic scattering events with an 'in–time' resolution of approximately 1 ns. By discriminating the out–of–time energy, beam gas and beam wall background events can already be rejected at the first trigger level.

8. PERFORMANCE OF THE SPACAL

The performance of final detector modules was tested in various test environments. The light yield of the detector was found to be (2.8 ± 0.3) photoelectrons/ MeV by comparison with a LED. The detector response to minimum ionizing particles is equivalent to 400 MeV. The modules were submitted to beam measurements at the CERN SPS and PS beam lines as well as at DESY. In Figure 9 the energy resolution of one of the first final design modules is shown in dependence of the beam energy. The module was tilted with respect to the beam direction by 3° horizontally and 3° vertically to avoid channeling. We determined the sampling term to be $(7.1 \pm 0.2)\%/\sqrt{E(\mathrm{GeV})}$ and the constant term to be $(0.6 \pm 0.2)\%$ if added in quadrature. Thus at electron energies of 30 GeV the resolution is well below 2% for fixed impact positions.

Horizontal and vertical scans across the module surface have been evaluated with the precise space information of a MWPC as reference. A space resolution of (2.8 ± 0.2) mm/ $\sqrt{E(\mathrm{GeV})} \oplus 0.4$ mm was determined.

The time resolution was measured at the CERN PS for 4 GeV electrons, interacting pions and minimum ionizing particles. The design time resolution of 1 ns was reached with the final electronics.

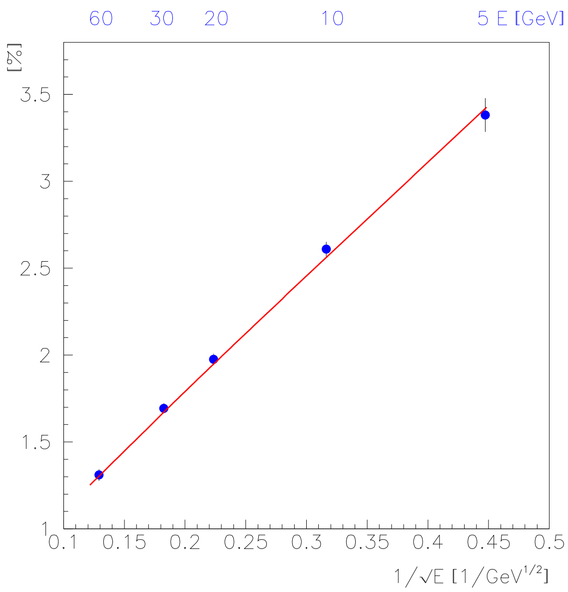

Figure 9. The energy resolution of a final calorimeter module as measured at the SPS at CERN.

During the production the quality of the detector modules was permanently monitored on a computer controlled β–source test bench built by the Institute LPNHE at the University of Paris VI and VII [11]. The collimated β–source is scanning in 1 to 2 mm steps across the front side of the modules moved by a high precision step motor. The resulting photomultiplier current is recorded. A typical example of the uniformity profile of a detector module presented as a lego plot is shown in the upper part of Figure 10.

The vertical coordinate corresponds to the normalized photomultiplier current, summed over all channels, the other axes indicate the β-source position. In the lower part of Figure 10 the projection to one of the space coordinates is shown. The border between to adjacent cells is indicated by the vertical line at an x value close to 20 mm. For this cell boundary the uniformity is excellent. Note, that the remaining fluctuations of a few per cent can entirely be explained by the light yield fluctuations of the individual fibers.

All standard supermodules and examples of all types of special modules were scanned with the test bench. The scan data should enable us to correct the local inhomogeneities observed at the boundary between some submodules. Inhomogeneities between the border of adjacent cells within a submodule are much less frequent and generally small.

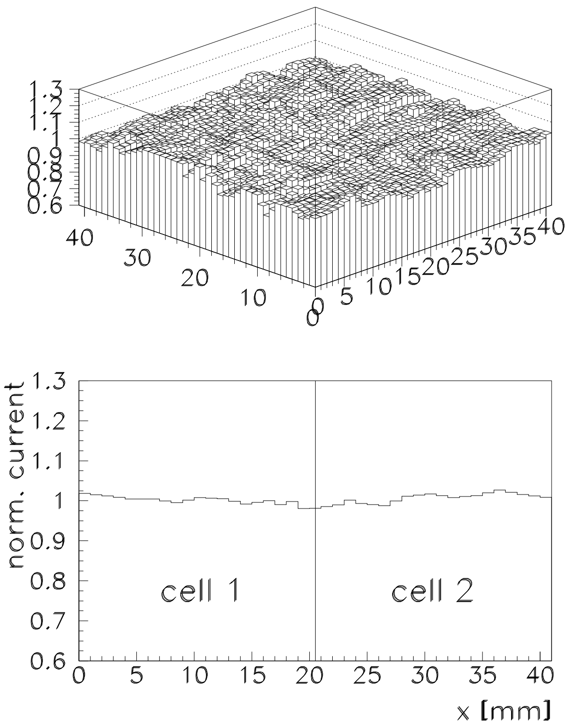

Figure 10. Uniformity profiles obtained with the β–source test bench. The current axis is strongly zero–suppressed

9. SUMMARY

The new spaghetti calorimeter of the H1 collaboration will be installed winter–shutdown 94/95 in the H1 detector. The detector combines compactness and good energy resolution. The lead to fiber ratio of 2:1 together with a fiber diameter of 0.5 mm is at the limit of what is technically possible. The H1 spaghetti calorimeter was designed and constructed within less than two years after its official proposal. The main design goals have, however, successfully been confirmed in both test beam and β–source measurements of final modules. We are looking forward to the first experience of operating the detector in genuine electron–proton collisions.

10. ACKNOWLEGDEMENTS

It is a pleasure to thank my colleagues and the many engineers and technicians from the participating institutes outside DESY for their outstanding commitment and their good team spirit. Their excellent work made the successful realization of the ambitious Spacal project possible. Many thanks to the organizers of the '94 Beijing Calorimetry Symposium' for the pleasant stay in China and the participation in their very interesting conference.

REFERENCES

1. J. Bartels and J. Feltesse, QCD at low x, Proceedings of the Workshop: Physics at HERA, DESY, Hamburg, Germany (1991).
2. H1 Collaboration, Technical Proposal to Upgrade the Backward Scattering Region of the H1 Detector, DESY PRC 93/02.
3. H1 Collaboration, Measurement of the Proton Structure Function $F_2(x, Q^2)$ in the Low x Region at HERA, Nucl. Phys. B407 (1993) 515.
4. R. D. Appuhn *et al.*, Electromagnetic Calorimetry with Lead Fluoride Crystals, Nucl. Instr. Meth. A 350 (1994) 208.

5. S. Dagoret *et al.*, Nucl. Instr. Meth. A 346 (1994) 137.
6. The KLOE collaboration, A general Purpose Detector for DAΦNE, LNF-92/-019 (1992).
7. J. Janoth *et al.*, Response of Mesh-Type Photomultiplier Tubes in Strong Magnetic Fields, Nucl. Instr. Meth. A 350 (1994) 221.
8. R. D. Appuhn *et al.*, Performance Tests with a Large Sample of fine Mesh Photomultipliers for Use at 1.2 Tesla, Proceedings of the IV International Conference on Calorimetry in High Energy Physics, La Biodola, Elba, Italy (1993).
9. A. Walther and R. Barschke, Studies of Scintillating Fibres for a Spaghetti Calorimeter to be used for the H1 Backward Upgrade Project, Proceedings of the Workshop on Scintillating Fiber Detectors, Notre Dame University, Indiana (1993).
10. R. Barschke, Diploma Thesis, University of Hamburg, Germany, unpublished (1994).
11. D. Lacour, Rapport de Stage DEA, LPNHE, Universites Paris VI et VII, September 1992.
12. F. Lehner, Diploma Thesis, University of Hamburg, Germany, unpublished (1994).
13. W. Stamm *et al.*, A low cost HV controller for PMTs, Nucl. Instr. Meth. A 328 (1993) 601.
14. B. Andrieu *et al.*, Nucl. Instr. Meth. A 336 (1993) 460.